

Wave-packet dynamics in a graphene with periodic potentials

M.M. Suleimanov,¹ M.U. Nosirov,¹ H.T. Yusupov,² A. Chaves,³ G.R. Berdiyurov,⁴ and Kh.Yu. Rakhimov^{1,5,*}

¹*Institute of Materials Science, Uzbekistan Academy of Sciences,
2-B Chingiz Aitmatov St., Tashkent 100084, Uzbekistan*

²*Department of Exact Sciences, Kimyo International University in Tashkent,
156 Shota Rustaveli St., Tashkent 100121, Uzbekista*

³*Departamento de Física, Universidade Federal do Ceará,
Caixa Postal 6030, Campus do Pici, 60455-900 Fortaleza, Ceará, Brazil*

⁴*Qatar Environment and Energy Research Institute, Hamad Bin Khalifa University, Doha, Qatar*

⁵*Tashkent International University of Education,
31 Imam Bukhariy St., Tashkent 100207, Uzbekistan*

(Dated: November 6, 2024)

We use the Dirac continuum model to study the propagation of electronic wave packets in graphene with periodically arranged circular potential steps. The time propagation of the wave packets are calculated using the split-operator method for different size, height and separation of the barriers. The time propagation of the wave packets is calculated using the split-operator method for various barrier sizes, heights, and separations. We found that, despite the pronounced Klein tunneling effect in graphene, the presence of a lattice of defects significantly impacts the propagation properties of the wave packets. For example, depending on the height and size of the incident wave packet, the transmission probability can decrease by more than 20%. The alteration of the polarity of the potential barriers also contributes to the transmission probabilities of the wave packet in graphene. The obtained results could provide valuable insights into the fundamental understanding of charge carrier dynamics in graphene-based nanodevices.

I. INTRODUCTION

Graphene is considered the most promising among 2D nanostructures for nanoelectronics applications, mainly due to its mechanical and thermal stability and exceptionally high carrier mobility and flux [1–5]. However, chemically synthesized graphene, however, frequently displays various structural irregularities, such as grain boundaries, vacancies, dislocations, impurity atoms, and defects arising from changes in carbon hybridization [6–8]. Consequently, these defects significantly affect graphene’s structural stability, electronic and transport properties, optical characteristics, and other observable features, as even slight modifications to the honeycomb arrangement of carbon atoms can drastically impact these properties [9–11]. Therefore, understanding the dynamics of charge carriers in the presence of structural defects is of practical importance for the development of graphene-based nanoelectronic components.

In this work, we use numerical simulations to investigate wave packet propagation in graphene with periodic scalar electric potentials. These wave packets can scatter off such defects, ultimately influencing the material’s conductance [12–20]. Extensive research has been conducted to study wave packet propagation within the Dirac-Weyl Hamiltonian in pristine graphene, graphene with various dopants [15, 16], and under uniform external magnetic fields [21–24]. However, theoretical studies on wave packet propagation through potential barriers

remain limited [25–32]. In this study, we model a periodic lattice of circular charged regions (electron-rich and hole-rich puddles) that can form in graphene due to inherent disorder [33, 34]. We implement Dirac continuum model to understand the effect of such an disorder for the transmission of electrons in graphene. This method was successfully applied recently to study the wave-packet propagation in graphene in the presence of randomly distributed electric potentials [35, 36]. We found that, despite overall charge neutrality, the presence of such a periodic lattice significantly affects wave packet propagation in graphene. For instance, depending on the parameters of the wave packet, such as its energy, the transmission probability (P) can be reduced by up to 30%.

II. MODEL SYSTEM AND THEORETICAL FRAMEWORK

Figure 1 illustrates our model systems, which comprise a graphene monolayer with lateral dimensions $L = 1024$ nm and $W = 128$ nm, featuring a periodic arrangement of scalar electric potentials. In this figure each circular dot with radius R mimic the presence of electron and hole puddles in real graphene samples, where these puddles appear with equal probability for both electrons and holes. To model this, we use scattering centers alternating between positive ($+V_0$) and negative ($-V_0$) potentials, representing regions with locally higher electron (in negative potential) or hole (in positive potential) densities, while maintaining a net zero average potential across the entire scattering region. The separation of the dots in the direction perpendicular to the wave packet propa-

*Electronic address: kh.rakhimov@gmail.com

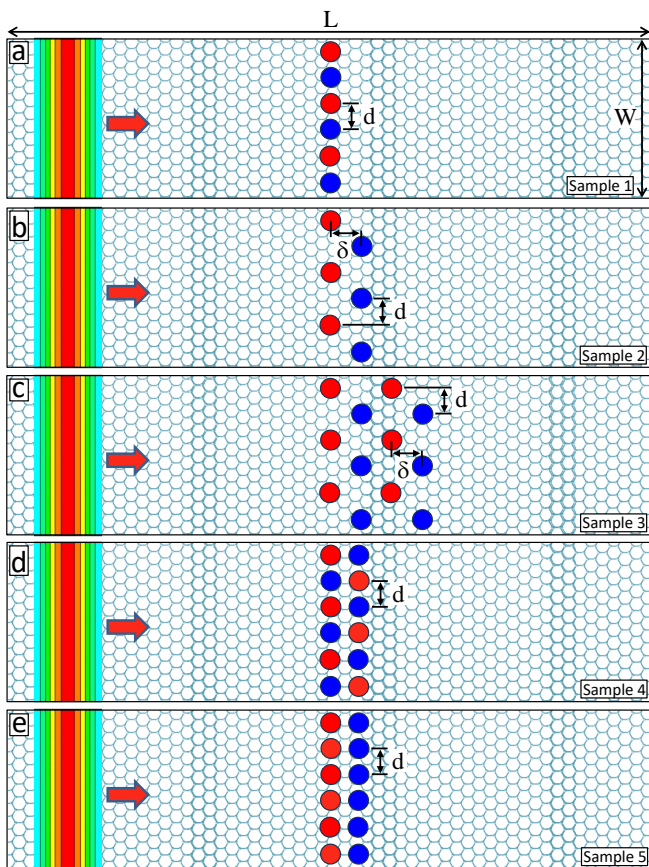


FIG. 1: The schematic illustration of wave packet propagation in graphene along the forward direction (indicated by an arrow) in the presence of periodically arranged circular potentials. The red and blue dots represent regions with positive and negative potentials, respectively.

gation is $d = 21.3$ nm for all the samples considered. For samples 2 and 3, the barriers are separated by a distance of $\delta = 6R$ along the wave packet propagation, while for samples 4 and 5, this separation is $\delta = 3R$. An electron wave packet is modeled as a Gaussian wave front

characterized by energy E and width a_x .

As initial wave packet, we consider a gaussian wave front, namely, a wave packet that is constant the y -direction, but which has a width a_x in the x -direction, multiplied by a pseudo-spinor $(1 \ i)^T$ and by a plane wave

$$\Psi(x, y, 0) = N \begin{pmatrix} 1 \\ i \end{pmatrix} e^{ikx - \frac{x^2}{2a_x^2}} \quad (1)$$

where N is a normalization constant and k is the wave vector, which, in graphene, is related to the wave packet energy E by $k = E/\hbar v_F$, where v_F is the Fermi velocity. The choice of the pseudo-spinor is made so that $\langle \sigma_x \rangle = 1$ and $\langle \sigma_y \rangle = \langle \sigma_z \rangle = 0$, which guarantees a wave packet propagation along the x -direction [37]. Moreover, we choose to work with a wave front, instead of a circularly symmetric wave packet, in order to avoid *zitterbewegung* (a trembling motion of the wave packet) [37, 38] along the y -direction. All the results in the remainder of this paper are obtained for a wave packet with energy $E = 100$ meV and widths $a_x = 100, 150$ and 200 nm.

The propagation of the wave packet is performed by applying the time-evolution operator on the initial wave packet

$$\Psi(x, y, t + \Delta t) = e^{-\frac{i}{\hbar} H \Delta t} \Psi(x, y, t) \quad (2)$$

where the Hamiltonian H , assumed to be time-independent, is the one for low energy electrons in graphene

$$H = v_F (\vec{\sigma} \cdot \vec{p}) + V(x, y) \mathbf{I}, \quad (3)$$

where $\vec{\sigma}$ is the usual Pauli vector, \mathbf{I} is the 2×2 identity matrix and the wave functions are written as pseudo-spinors $\Psi = (\Psi_A, \Psi_B)^T$, where Ψ_A (Ψ_B) is the probability of finding the electron in the sub-lattice A (B) of graphene. We separate the potential and kinetic energy terms of the time-evolution operator through the split-operator technique [39, 40],

$$\exp \left[-\frac{i}{\hbar} H \Delta t \right] = \exp \left[-\frac{i}{2\hbar} V(x, y) \mathbf{I} \Delta t \right] \exp \left[-\frac{i}{\hbar} v_F \vec{p} \cdot \vec{\sigma} \Delta t \right] \exp \left[-\frac{i}{2\hbar} V(x, y) \mathbf{I} \Delta t \right], \quad (4)$$

where terms of order higher than $O(\Delta t^3)$ are neglected as an approximation. The advantage of such separation is that it allows us to perform multiplications in real and reciprocal spaces separately, so that we avoid writing the momentum operator as a derivative just by making a Fourier transform of the functions and writing $\vec{p} = \hbar \vec{k}$. Furthermore, the exponentials of Pauli matrices terms

can be re-written exactly as matrices [27], which simplifies even more the calculations. We perform wave packet propagations with a time step as small as $\Delta t = 0.1$ fs and keep track of the probabilities of finding the electron before and after the scattering region. The latter probability can also be seen as a transmission probability (P) through the scattering region.

Notice that performing a Fourier transform while solv-

ing Eq. (4) necessarily imposes a periodic boundary condition to our system. Thus, in order to avoid spurious reduction (enhancement) of the transmission (reflection) probability, we consider a very long grid in the propagation direction, with an area $128 \text{ nm} \times 1024 \text{ nm}$, whereas the scattering centers are distributed within an area of $A = 128 \text{ nm} \times 40 \text{ nm}$ around the $x = 0$ axis. Periodic boundary conditions are applied in both lateral directions and the wave packets are propagated with a time step of 0.1 fs. The probabilities are calculated before and after the areas with barriers, where the latter one is considered as a transmission probability of the wave packet. All simulations were performed at a wave packet energy of $E = 100 \text{ meV}$ to ensure the method remains within its applicable range.

III. RESULTS AND DISCUSSIONS

As a reference to our further studies, we first investigate the case where the potential barriers are periodically arranged in the direction perpendicular to the wave packet propagation without any shift $\delta = 0$ (sample 1, see Fig. 1(a)). Figure 2 presents the transmission probabilities P of the wave packet as a function of time for different values of the barrier height $|V_0|$. For smaller radius of the dots, the transmission probability decreases with increasing the barrier height (see Fig. 2 (a)). With increasing the size of the barrier, non-monotonic dependence of P on $|V_0|$ is obtained (Fig. 2 (b)). For example, the transmission probability for $|V_0| = 200| \text{ meV}$ is higher than that for $|V_0| = 150| \text{ meV}$. The effect of the barriers on the dynamics of the wave packet becomes more pronounced for wider wave packets, as shown in Figs. 2 (c,d). For this particular wave packet width, a non-monotonic dependence of P on the barrier height is observed even for the smallest considered dot size (Fig. 2(c)). Panels 1-5 in the inset of Fig. 2 (c) illustrate the wave packet's propagation dynamics through the barrier area. Although the transmission probability of the wave packet is high ($P > 80\%$) for the chosen parameters, significant distortion occurs within the defect area.

Figure 3 shows the transmission probabilities of the wave packet in sample 2, where dots of the same potential polarity are shifted by a distance of $\delta = 6R$ relative to the dots of opposite polarity (refer to Fig. 1(b)). Two main differences are observed when comparing these results with those of sample 1. First, the transmission probabilities of the wave packet decrease across all considered values of V_0 in sample 2. This suggests a higher level of wave packet scattering or potential barrier impacts in this configuration. Second, additional features emerge on the probability curves, indicating complex interactions within the sample that may influence the wave packet's behavior. This is illustrated in panels 1-3 of the inset in Figure 3, where snapshots of the wave packet distribution are plotted at times corresponding to the peculiarities observed on the probability curve. For example,

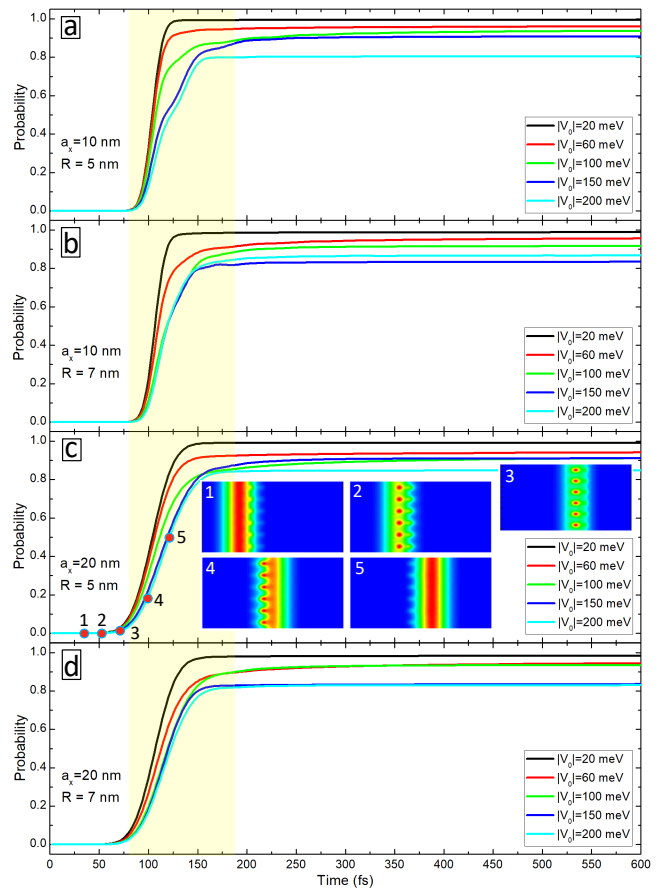


FIG. 2: Transmission probabilities of the wave packet as a function of time for Sample 1, for different values of the barrier height $|V_0|$. The wave packet width is $a_x = 10 \text{ nm}$ (a, b) and $a_x = 20 \text{ nm}$ (c,d), while the dot radius is $R = 5 \text{ nm}$ (a,c) and $R = 7 \text{ nm}$ (b,d). The shaded areas highlight the transmission probabilities when the wave packet is within the defected region. Insets in (c) shows the snapshots of the wave-packet propagation for parameters $a_x = 20 \text{ nm}$ and $R = 5 \text{ nm}$ at times indicated on the probability curve for $|V_0| = 200 \text{ meV}$.

the minimum observed on the probability curve (point 2) corresponds to the wave packet scattering from the second row of dots. A large portion of the wave packet will be reflected by the defected area, thereby reducing the overall transmission of the wave packet. Thus, the dynamics of the wave packet are significantly influenced by the simple act of shifting dots with the same potential polarity, as evidenced by decreased transmission probabilities, increased scattering, and the emergence of additional complex features in the probability curves.

The transmission probability decreases further as the number of scattering centers increases, due to the prolonged interaction between the wave packet and the defects. This is illustrated in Fig. 4 for sample 3, which includes an additional row of dots that are mutually shifted (see Fig. 1 (c)). Reduced transmission is particularly noticeable when the wave packet is within the defected

region, where defects disrupt its propagation. This reduction occurs due to the scattering and interference caused by the irregularities. As the barrier height increases, the transmission probabilities further decrease, as observed in previous cases. A higher barrier height leads to increased reflection and scattering of the wave packet, making it more difficult for the packet to tunnel through the defected region, thereby reducing the overall transmission.

Figure 5 summarizes our findings on how the rearrangement of potential defects affects the wave packet dynamics in graphene. The figure presents the transmission probability of the wave packet as a function of barrier height V_0 for samples 1-3, illustrating the influence of different defect configurations on the transmission behavior. The most apparent effect of the defect rearrangement is a reduction in the wave packet's transmission. For instance, the transmission probability decreases from 0.8 in sample 1 to 0.6 in sample 3, highlighting the impact of the defect arrangement on the wave packet's ability to transmit. Secondly, the effect of the dot size becomes more pronounced as the spacing between the dots increases. For example, in sample 1, the maximum difference in transmission probability between dot radii of $R = 5$ nm and $R = 7$ nm is 0.08. In contrast, for sample 3, the same difference is more pronounced, reaching 0.22. In configurations where the dots are more sparsely distributed, the wave packet interacts with each defect individually for a longer duration, amplifying the influence of the dot size on transmission. Larger dots create stronger scattering potentials, which significantly disrupt the wave packet's trajectory and reduce transmission probabilities. In contrast, when the dots are closely spaced, the individual impact of each dot is less distinct, and the overall transmission behavior is more dominated by the collec-

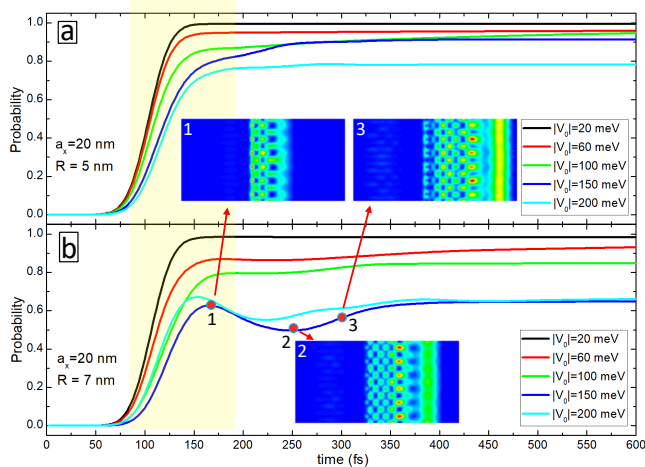


FIG. 3: Probabilities of finding the electron after the barrier region as a function of time for Sample 2, for different values of the barrier height $|V_0|$. Insets show the snapshots of the wave-packet propagation for parameters $a_x = 20$ nm and $R = 7$ nm at times indicated on the probability curve for $|V_0| = 150$ meV.

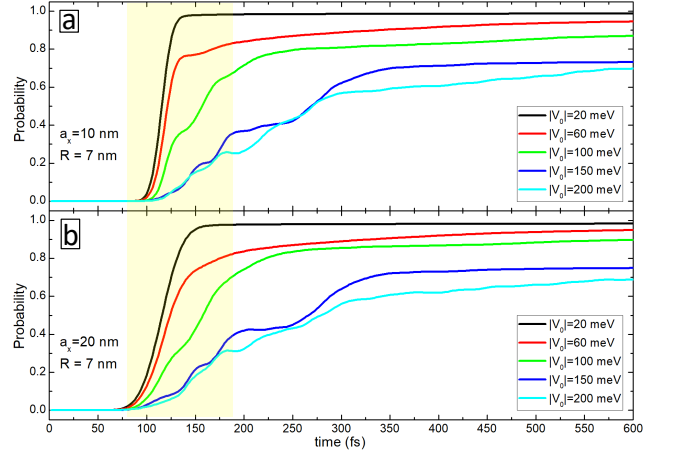


FIG. 4: Transmission probabilities of the wave packet as a function of time for Sample 3 for different values of the barrier height $|V_0|$. The radius of the dots is $R = 7$ nm and the width of the wave packet is $a_x = 10$ nm (a) and $a_x = 20$ nm (b).

tive scattering effect of the entire defected region.

Finally, we explore the impact of potential polarity alterations on the dynamics of the wave function, as demonstrated in the cases of samples 4 and 5. Sample 4 features a symmetric vertical arrangement of alternating potentials, whereas Sample 5 presents a staggered, zigzag pattern, introducing asymmetry in the wave packet's in-

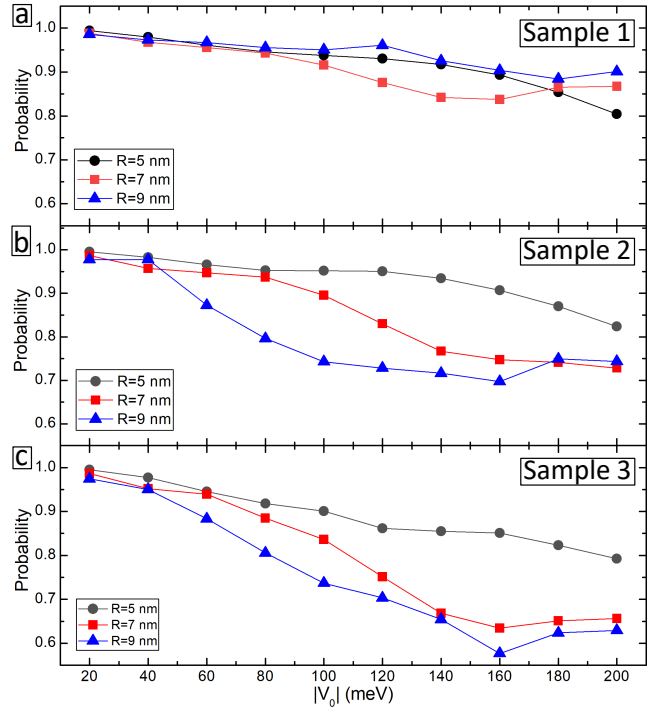


FIG. 5: Transmission probabilities of the wave packet in sample 1 (a), 2 (b) and 3 (c) as a function of barrier height $|V_0|$ for three different values of the dot radius. The width of the wave packet is set to $a_x = 10$ nm.

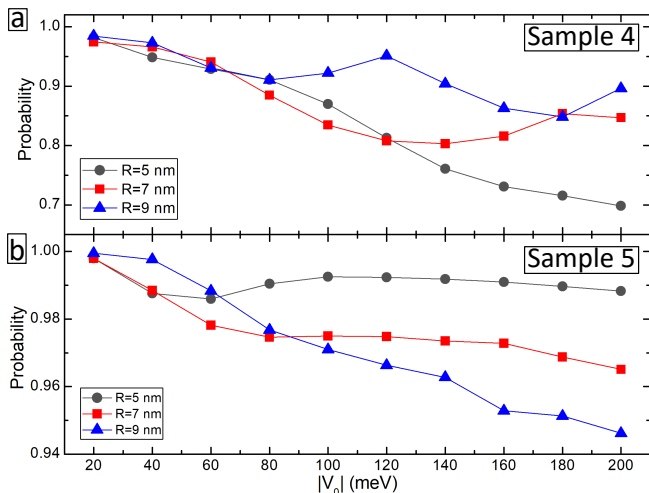


FIG. 6: Transmission probabilities of the wave packet in sample 4 (a) and 5 (b) as a function of energy for three different values of the dot radius. The width of the wave packet is set to $a_x = 10$ nm.

interaction with the potential barriers. Figure 6 presents the transmission probabilities of the wave packet as a function of the barrier height V_0 for these sample for three different dot sizes. This comparison highlights how the barrier height and dot size influence the transmission behavior in each sample. This variation in arrangement leads to distinct transmission and scattering behaviors

between the two samples. Interestingly, for Sample 4, the transmission probability increases with the radius of the dots at higher values of V_0 (see Fig. 6(a)). In contrast, for Sample 5, an increase in the dot size leads to a reduction in transmission probabilities. This opposing trend highlights the distinct influence of the dot arrangement on how the wave packet interacts with the potential barriers in each sample.

IV. CONCLUSIONS

In this work, we used the Dirac continuum model to study the propagation of electronic wave packets in graphene with periodically arranged potential barriers. Our simulations reveal that both the size and arrangement of the scattering centers significantly affect transmission probabilities. Increasing the barrier height leads to non-monotonic changes in transmission, with larger wave packets being more impacted. The arrangement of potential barriers, whether symmetric or staggered, plays a crucial role, with staggered configurations reducing transmission more effectively. These findings enhance our understanding of wave packet dynamics in graphene and could inform the design of graphene-based electronic devices.

V. ACKNOWLEDGEMENTS

-
- [1] K. S. Novoselov, A. K. Geim, S. V. Morozov, D. Jiang, Y. Zhang, S. V. Dubonos, I. V. Grigorieva, and A. A. Firsov, Electric field effect in atomically thin carbon films, *Science* 306 (2004) 666.
- [2] A. K. Geim and K. S. Novoselov, The rise of graphene, *Nat. Mater.* 6 (2007) 183.
- [3] A. K. Geim, Graphene: Status and Prospects, *Science* 324 (2009) 1530-1534.
- [4] A. H. Castro Neto, F. Guinea, N. M. R. Peres, K. S. Novoselov, and A. K. Geim, The electronic properties of graphene, *Rev. Mod. Phys.* 81 (2009) 109.
- [5] K. S. Novoselov, V. I. Fal'ko, L. Colombo, P. R. Gellert, M. G. Schwab, and K. Kim, A roadmap for graphene, *Nature* 490 (2012) 192.
- [6] M. H. Gass, U. Bangert, A. L. Bleloch, P. Wan, R. R. Nair, and A. K. Geim, Free-standing graphene at atomic resolution, *Nature Nanotechnology* 3 (2008) 676-681.
- [7] J. C. Meyer, C. Kisielowski, R. Erni, M. D. Rossell, M.F. Crommie, and A. Zettl, Direct Imaging of Lattice Atoms and Topological Defects in Graphene Membranes, *Nano Lett.* 8 (2008) 3582-3586.
- [8] A. Eckmann, A. Felten, A. Mishchenko, L. Britnell, R. Krupke, K. S. Novoselov, and C. Casiraghi, Probing the Nature of Defects in Graphene by Raman Spectroscopy, *Nano Lett.* 12 (2012) 3925-3930.
- [9] A. Hashimoto, K. Suenaga, A. Gloter, K. Urita, S. Iijima, Direct evidence for atomic defects in graphene layers, *Nature* 430 (2004) 870.
- [10] F. Banhart, J. Kotakoski, and A. V. Krasheninnikov, Structural Defects in Graphene, *ACS NANO* 5 (2011) 26-41.
- [11] R. H. Telling and M. I. Heggie, Radiation defects in graphite, *Philos. Mag.* 87 (2007) 4797-4846.
- [12] F. Banhart, J. Kotakoski, and A. V. Krasheninnikov, Structural defects in graphene, *ACS Nano* 5 (2011) 26-41.
- [13] Z. Lin, B. R. Carvalho, E. Kahn, R. Lv, R. Rao, H. Terrones, M. A. Pimenta, and M. Terrones, Defect engineering of two-dimensional transition metal dichalcogenides, *2D Mater.* 3 (2016) 022002.
- [14] J. Jiang, T. Xu, J. Lu, L. Sun, and Z. Ni, Defect Engineering in 2D Materials: Precise Manipulation and Improved Functionalities, *Research* 2019 (2019) 4641739.
- [15] Kh. Yu. Rakhimov, A. Chaves, and P. Lambin, Scattering of Dirac electrons by randomly distributed nitrogen substitutional impurities in graphene. *Appl. Sci.* 6 (2016) 256.
- [16] P. Vancso, A. Mayer, P. Nemes-Incze, and G.I. Mark. Wave Packet Dynamical Simulation of Quasiparticle Interferences in 2D Materials, *Appl. Sci.* 11 (2021) 4730.
- [17] J.-H. Chen, W. G. Cullen, C. Jang, M. S. Fuhrer, and E. D. Williams, Defect Scattering in Graphene, *Phys. Rev. Lett.* 102 (2009) 236805.
- [18] Q. Yu, L. A. Jauregui, W. Wu, R. Colby, J. Tian, Z. Su, H. Cao, Z. Liu, D. Pandey, D. Wei, et al., Control and

- characterization of individual grains and grain boundaries in graphene grown by chemical vapour deposition, *Nat. Mater.* 10 (2011) 443-449.
- [19] H. Qiu, T. Xu, Z. Wang, W. Ren, H. Nan, Z. Ni, Q. Chen, S. Yuan, F. Miao, F. Song, et al., Hopping transport through defect-induced localized states in molybdenum disulphide, *Nat. Commun.* 4 (2013) 2642.
- [20] M. Andelkovic, K. Y. Rakhimov, A. Chaves, G. R. Berdiyrov, and M. V. Milosevic, Wave-packet propagation in a graphene geometric diode *Physica E* 147 (2023) 115607.
- [21] T. M. Rusin and W. Zawadzki, Zitterbewegung of electrons in graphene in a magnetic field, *Phys. Rev. B* 78 (2008) 125419.
- [22] T. M. Rusin and W. Zawadzki, Theory of electron Zitterbewegung in graphene probed by femtosecond laser pulses, *Phys. Rev. B* 80 (2009) 045416.
- [23] G. M. Maksimova, V. Ya. Demikhovskii, and E. V. Frolova, Wave packet dynamics in a monolayer graphene, *Phys. Rev. B* 78 (2008) 235321.
- [24] E. Romera and F. de los Santos, Revivals, classical periodicity, and zitterbewegung of electron currents in monolayer graphene, *Phys. Rev. B* 80 (2009) 165416.
- [25] H. Nitta, T. Kudo, and H. Minowa, Motion of a wave packet in the Klein paradox, *Am. J. Phys.* 67 (1999) 966.
- [26] J. M. Pruneda and I. Souza, Nonadiabatic wavepacket dynamics: k -space formulation, *Phys. Rev. B* 79 (2009) 045127.
- [27] Kh. Yu. Rakhimov, A. Chaves, G. A. Farias, and F. M. Peeters, Wavepacket scattering of Dirac and Schrödinger particles on potential and magnetic barriers, *J. Phys.: Condens. Matter* 23 (2011) 275801.
- [28] B. Balzer, S. Dilthey, G. Stock, and M. Thoss, Quasiclassical and semiclassical wave-packet dynamics in periodic potentials, *J. Chem. Phys.* 119 (2003) 5795-5804.
- [29] Th. Anker, M. Albiez, B. Eiermann, M. Taglieber, and M. K. Oberthaler, Linear and nonlinear dynamics of matter wave packets in periodic potentials, *Optics Express* 12 (2004) 11-18.
- [30] H.M. Krenzlin, J. Budczies, and K.W. Kehr, Wave packet tunneling, *Ann. Phys. (Leipzig)* 7 (1998) 732.
- [31] A. B. Watson, J. Lu, and M. I. Weinstein, Wavepackets in inhomogeneous periodic media: Effective particle-field dynamics and Berry curvature, *J. Math. Phys.* 58 (2017) 021503.
- [32] A. Watson and M. I. Weinstein, Wavepackets in Inhomogeneous Periodic Media: Propagation Through a One-Dimensional Band Crossing, 363 (2018) 655-698.
- [33] J. Martin, N. Akerman, G. Ulbricht, T. Lohmann, J. H. Smet, K. von Klitzing, and A. Yacoby, Observation of electron-hole puddles in graphene using a scanning single-electron transistor, *Nat. Phys.* 4 (2008) 144.
- [34] G. Schubert and H. Fehske, Metal-to-insulator transition and electron-hole puddle formation in disordered graphene nanoribbons, *Phys. Rev. Lett.* 108 (2012) 066402.
- [35] S. Palpacelli, M. Mendoza, H. J. Herrmann, and S. Succi, Klein tunneling in the presence of random impurities, *Int. J. Mod. Phys.* 23 (2012) 1250080.
- [36] Kh. Yu Rakhimov, A. Chaves, G.A. Farias, Wave packet propagation through randomly distributed scattering centers in graphene. Book chapter in *Low-Dimensional Functional Materials*, Springer 2013, Pages 119-126.
- [37] A. Chaves, L. Covaci, Kh. Yu. Rakhimov, G. A. Farias, and F. M. Peeters, Wave-packet dynamics and valley filter in strained graphene, *Phys. Rev. B* 82 (2010) 205430.
- [38] T. M. Rusin and W. Zawadzki, Zitterbewegung of relativistic electrons in a magnetic field and its simulation by trapped ions, *Phys. Rev. D* 82 (2010) 125031.
- [39] M. H. Degani and J. P. Leburton, Single-electron states and conductance in lateral-surface superlattices, *Phys. Rev. B* 44 (1991) 10901.
- [40] M. Suzuki, Fractal decomposition of exponential operators with applications to many-body theories and Monte Carlo simulations, *Phys. Lett. A* 146 (1990) 319-323.